Special Issue on "Theoretical and Computational Chemistry"

J. Indian Chem. Soc.,
Vol. 96, July 2019, pp. 1011-1017

First principles investigation of atomic gold dispersed g-C_3N_4 as an active catalyst for CO oxidation reaction

Ananth Kandala[a] and K. Srinivasu*[b,c]

[a]School of Physics, University of Hyderabad, Hyderabad-500 046, India

[b]Theoretical Chemistry Section, Bhabha Atomic Research Centre, Mumbai-400 085, India

[c]Homi Bhabha National Institute, Mumbai-400 094, India

E-mail: ksvasu@barc.gov.in

Manuscript received online 15 May 2019, revised and accepted 01 June 2019

Density functional theory calculations have been performed to explore atomic Au decorated graphitic carbon nitride (Au@g-C_3N_4) as an active catalyst for CO oxidation reaction. Binding energy of Au atom to the carbon nitride substrate is found to be sufficiently strong to prevent the aggregation of adsorbed metal atoms to form clusters. Binding energy of both the reactants over Au@g-C_3N_4 is significantly higher as compared to that of the product. CO oxidation over Au@g-C_3N_4 is demonstrated to follow the Langmuir-Hinshelwood (LH) mechanism initially and then through the Eley-Rideal (ER) mechanism. Minimum energy path for both the LH and ER steps has been investigated through nudge elastic band and dimer methods. Highest energy barrier for first CO_2 formation through LH step is calculated to be 44.19 kJ/mol whereas the second CO_2 formation by ER step is found to be almost barrier less. Strong interaction between the reactants and catalyst surface is attributed to the observed charge transfer from metal *d* states to the π^* states of reactants.

Keywords: CO oxidation reaction, density functional theory study, graphitic carbon nitride, single atom catalysts, gold catalysis.

Introduction

Emission of CO gas into the earth's atmosphere from vehicular exhausts, industrial processes, etc., is among the many major environmental concerns. One possible solution that received continues importance is the catalytic oxidation of CO to CO_2. During the last few decades, large number of studies has been carried out for making potential catalyst for CO oxidation reaction[1–5]. Noble metal based catalysts such as Pt, Pd, Ru, Rh and Au, have been shown to be active catalysts for CO oxidation and many other important reactions[6–9]. Unlike the other noble metals which require relatively high temperatures to catalyse the CO oxidation reaction, Au is shown to be active even at low temperatures[10]. However, these metals are highly expensive and hence the reduction of amount of catalyst required is important. Small gold clusters and their doped counterparts were well explored as efficient catalyst for low temperature CO oxidation reaction[11–14]. In particular, metal supported catalysts, where the metals are finely dispersed over a substrate are extensively studied and shown to have excellent catalytic activity[15–17]. Reducing the metal cluster size is found to enhance the catalytic activity due to increase in the number of surface metal atoms that can involve in the catalytic process.

Single atom catalysts (SACs), such as single atoms of noble metals Au, Pt, Pd dispersed on a suitable substrate, are shown to be efficient catalysts for CO oxidation[18–20]. Single metal atom is more desirable as a catalyst because of the high surface area with all the atoms available as active sites and thereby reducing the amount of the required catalyst. However, preventing these atoms from aggregation to form larger clusters is highly challenging. This can be achieved by placing the metal atoms on a suitable substrate with sufficiently high binding energy and diffusion barrier making these catalysts stable and experimentally realizable. Different metals and metal oxides are explored as substrates to anchor the SACs where the metal atoms are placed over

a metal surface through alloying or over oxide substrate through metal-oxygen bonds[21,22]. Apart from the metals and metal oxides, two-dimensional (2D) materials like graphene, graphitic carbon nitride, silicene, graphyne, MoS_2, h-BN, etc. are shown to be other promising substrates for designing efficient SACs[23–31]. Pristine graphene with all sp^2 carbons is not a suitable substrate due to the lower metal binding energies. However, graphene with defects is shown to be an efficient substrate with improved metal binding energy and higher metal diffusion barrier which can prevent the metal agglomeration over the substrate[32]. Li *et al.*[24] reported the Au decorated silicene as highly active catalyst for CO oxidation reaction using the first principles calculations. Lin *et al.*[28] investigated range of metal atoms dispersed over the hexagonal boron nitride nano-sheets and concluded that the observed catalytic activity is due to the strong mixing between the metal 3*d* states and oxygen 2*p* states. Wu *et al.*[30] carried a systematic study of CO oxidation over Fe decorated graphyne and the results indicate that the metal atoms are strongly bonded over the graphyne substrate with high diffusion barrier and the CO oxidation proceeds through the Eley-Rideal (ER) mechanism.

In the present study, we explored single Au atom supported over g-C_3N_4 for its catalytic activity towards the CO oxidation reaction using the first principles calculations. Recent theoretical and experimental reports on metal decorated carbon nitride based materials for different catalytic applications such as water splitting, CO_2 reduction etc.[33–35] encourage us to select g-C_3N_4 as substrate for anchoring Au atoms. In our earlier studies we reported graphitic carbon nitride and its doped counterparts as efficient catalysts for photocatalytic water splitting reaction[36–38]. Samanta *et al.*[39] deposited Au nanoparticles on g-C_3N_4 and found significant enhancement in the photocatalytic activity for hydrogen production. Silver nanoparticle anchored g-C_3N_4 nanostructures were prepared by Khan *et al.*[40] and the nanostructures were shown to exhibit antimicrobial activity as well as photodegradation of dyes under visible light. Wang *et al.*[41] studied the oxygen evolution reaction over the plasmonic Au nanoparticles decorated g-C_3N_4.

Computational details

All the spin polarized periodic density functional theory (DFT) calculations were carried out using the plane wave based electronic structure code, Vienna Ab initio Simulation Package (VASP)[42,43]. Kohn-Sham equations of the valence electrons are being expanded using the plane-wave basis sets with a kinetic energy cut-off of 550 eV. Projector augmented wave (PAW) potentials were used to treat the interaction between the core and valence electrons[44,45]. Generalized Gradient Approximation (GGA) of Perdew-Burke-Ernzerhof (PBE) has been used to treat the exchange-correlation energy density functional[46]. van der Waals interactions have been incorporated using the dispersion corrections to the total energies using the Grimme's D3 semi-empirical method (PBE-D3)[47]. Brillouin zone has been sampled using a 3×3×1 automatically generated k-point mesh through Monkhorst-Pack method[48]. Electronic optimization was carried out through self-consistent field iterations with an energy cut-off of 1×10^{-6} eV. Both unit cell and atomic positions were relaxed to optimize all the reaction intermediates by setting a force cut-off of 0.005 eV $Å^{-1}$ on each atom. Minimum energy path and transition state of CO oxidation reaction have been investigated through the climbing image nudge elastic band and Dimer methods by implementing the transition state tools developed for VASP code[49–53]. Graphical software VESTA has been used for generating the reported figures[54]. Binding energy (BE) of an adsorbate (ads) over the substrate (sub) is calculated as

$$BE = E_{(ads+sub)} - [E_{(ads)} + E_{(sub)}] \quad (1)$$

where, $E_{(ads+sub)}$, $E_{(ads)}$ and $E_{(sub)}$ represents the energy of adsorbed system, free adsorbate and substrate respectively.

Results and discussion

To model the Au metal decorated g-C_3N_4, we considered the 2×2×1 super cell of g-C_3N_4 substrate containing 24 carbon and 32 nitrogen atoms as shown in Fig. 1(a). The structure consists of heptazine units connected through tertiary amine forming voids of nitrogen atoms that can bind the metal atoms. The optimized cell parameter is found to be 13.86 Å with C-N bond distances in the range of 1.322–1.457 Å. Different possible adsorption sites for adsorption of Au atom over the g-C_3N_4 surface have been considered and the minimum energy structure is shown in Fig. 1(b). Shortest Au-N distance is found to be 2.139 Å and the calculated metal binding energy to the surface is –164.31 kJ/mol. The strong binding of Au over the substrate indicates the stability of Au@g-C_3N_4 against metal aggregation. Bonding between Au and surface nitrogen atoms can also be explained from

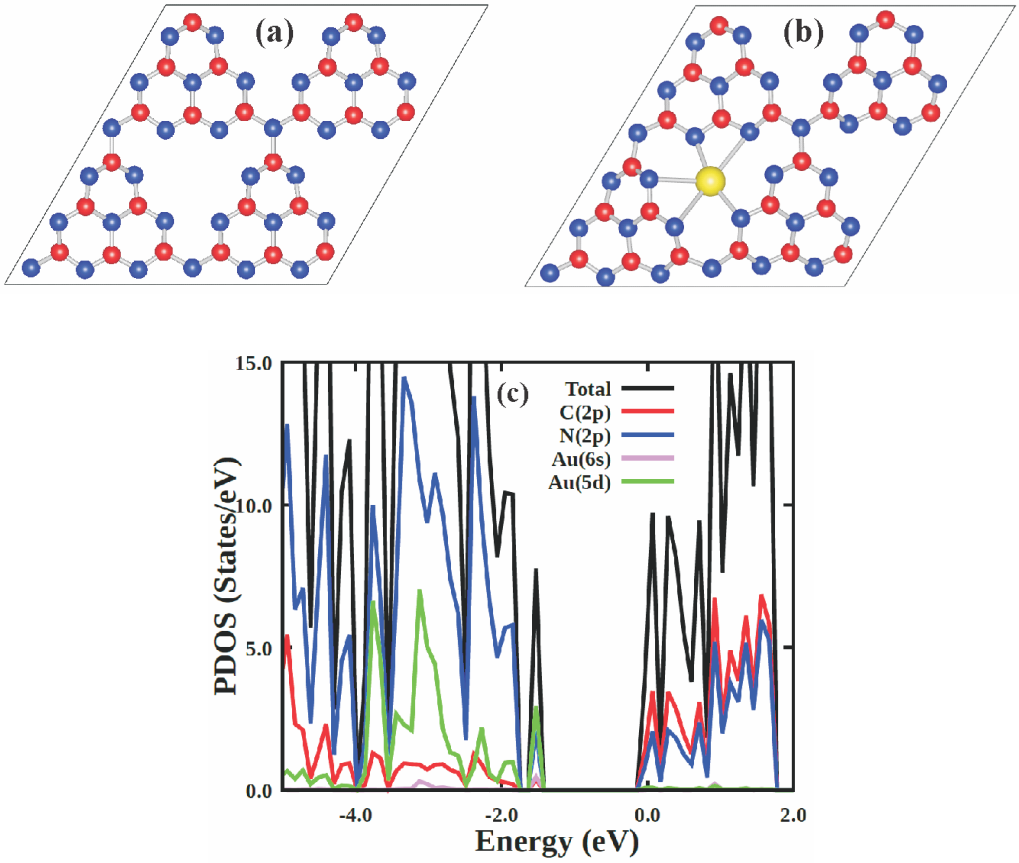

Fig. 1. Optimized super cell structure of (a) g-C_3N_4 and (b) Au@g-C_3N_4 along with the (c) density of states of Au@g-C_3N_4.

the projected density of states (PDOS) reported in Fig. 1(c) where there is a significant overlap between the Au (5*d* and 6*s*) states and N 2*p* states near the valance band maxima. Another important observation from the DOS plot is the shifting of Fermi level to the conduction band which can be attributed to the charge transfer from metal to the π^* states of the substrate. To verify this, we have also measured the extent of charge transfer between the Au atom and the substrate using the Bader charge density analysis[55]. The results reveal that the adsorbed Au atom carries a partial positive charge of 0.48 resulting from the electron transfer from metal *d* states to substrate π^* states indicating the strong bonding between the Au atom and g-C_3N_4.

Before exploring the CO oxidation reaction mechanism, we discuss the adsorption energetics of both the reactants and product over the Au@g-C_3N_4 substrate. Minimum energy structures of O_2, CO and CO_2 adsorbed Au@g-C_3N_4 are reported in Figs. 2(a), 2(b) and 2(c) respectively. For the case of O_2 adsorption, we considered both side-on and end-on orientations and both are optimized to the same configuration as reported in Fig. 2(a). The O-O and Au-O bond distances in minimum energy configuration are found to be 1.316 Å and 2.012 Å respectively. The elongation of O-O bond length from 1.233 Å in free O_2 molecule indicates strong interaction between O_2 and catalyst substrate and the calculated binding energy is found to be –118.68 kJ/mol. The increase in O-O distance can be attributed to the charge transfer from substrate to O_2 anti-bonding orbitals as discussed in earlier reports[24]. To verify this, we calculated the atomic charges and found that there is a net charge transfer of 0.483 e from Au@g-C_3N_4 to O_2. In the case of CO adsorbed system, CO is found to interact in an end-on configuration as shown in Fig. 2(b) with the C-O and Au-C bond distances of 1.148 Å and 1.876 Å respectively. The calculated binding energy of CO over Au@C_3N_4 is found to be –189.30 kJ/mol, which is considerably higher as compare to the O_2 binding energy. As for the case of CO_2 adsorption, the calculated binding energy is found to be –23.02 kJ/mol which is signifi-

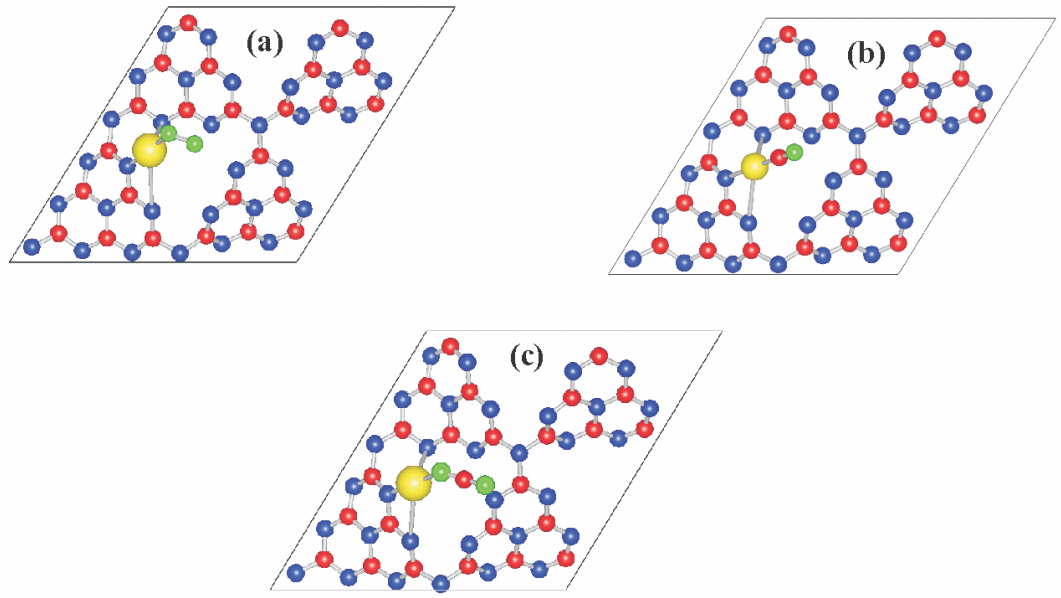

Fig. 2. Optimized super cell structures of (a) O_2, (b) CO and (c) CO_2 adsorbed Au@g-C_3N_4.

cantly lower as compared to that of both the reactants. In the adsorbed state, CO_2 is found to have two different C-O bond lengths (1.19 Å and 1.165 Å) and the O-C-O bond angle is measured to be 171.98° indicating the distortion from its linear structure in molecular form. The optimized Au-O bond distance is found to be 2.115 Å. These binding energies indicate that both the reactants of the CO oxidation reaction bind strongly as compared to the product indicating that the considered catalyst can be efficient for CO oxidation reaction.

To study the reaction mechanism of CO oxidation, it is important to understand the two well established mechanisms of CO oxidation reaction, namely Langmuir-Hinshelwood (LH) and Eley-Rideal (ER) mechanisms. In LH mechanism, both the reactants co-adsorb leading to the formation of a preoxo complex followed by the release of one CO_2 molecule as follows

$$* + CO + O_2 \rightarrow *OOCO \rightarrow *O + CO_2$$

where, * represents the substrate. In the case of ER mechanism, CO interacts with the dissociatively adsorbed oxygen over the catalyst and finally releasing the product as

$$*O + CO \rightarrow * + CO_2$$

However, since the O_2 is adsorbed in molecular form over the Au@g-C_3N_4, ER mechanism at the starting is difficult. To study the LH mechanism, we considered the CO adsorbed catalyst and allowed O_2 to co-adsorb since the CO binding energy is stronger as compared to O_2 binding.

The optimized initial structure (IS1) for CO and O_2 co-adsorption is shown in Fig. 3 with the shortest Au-O_2 and O_2-CO distances are found to be 3.335 Å and 3.598 Å respectively. In the transition state (TS1) for co-adsorption, O_2 molecules approaches closer with a shortest distance between the two reactant molecules is being 2.16 Å and the Au-O_2 distance is found to be 3.16 Å. In the final co-adsorbed metastable system (MS1), O_2 molecule is bonded to the adsorbed CO as shown in Fig. 3(d) with a C-O distance of 1.525 Å and still the Au-O distance is more than 3.0 Å. To calculate this MEP, we considered 8 images between the initial and final states for NEB calculation. To locate the transition state more precisely, we used the Dimer method. The calculated energy barrier for co-adsorption of O_2 over CO adsorbed Au@g-C_3N_4 is found to be 33.77 kJ/mol. From MS1 structure, formation of surface adsorbed O atom and free CO_2 molecule as final states (FS1) passes through a transition state (TS2) and both these structures are presented in Fig. 3. In the optimized TS2, the O-O distance is found to

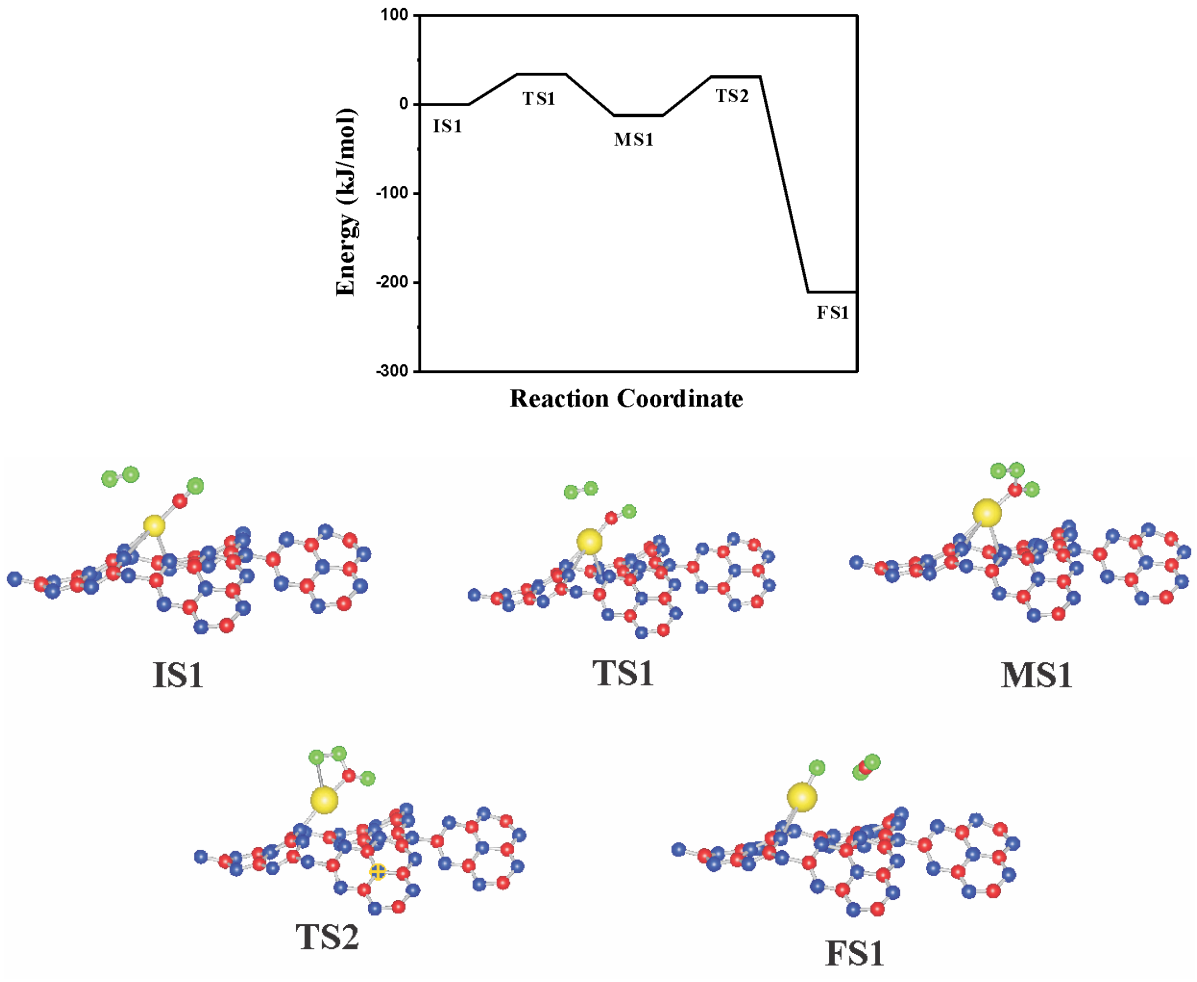

Fig. 3. Energy profiles in the LH mechanism along with the corresponding optimized states (IS1, TS1, MS1, TS2, and FS1).

increase to 1.438 Å from 1.329 Å in MS1 structure. The Au-O bond distance in TS2 is found to be 2.465 Å which is 3.002 Å in MS1. In case of FS, the Au-O distance is found to further shrink to 1.783 Å with the CO_2 molecules formed separated away (3.796 Å) from the active site. For calculating the energy barrier, we initially considered 8 images and fine-tuned by considering 8 more images near the saddle point due to the longer band. Finally Dimer method is used to locate the TS2 and the calculated energy barrier for CO_2 release is found to be 44.19 kJ/mol. Full energy profiles for the first step of CO oxidation by LH mechanism is shown in Fig. 3.

After the formation of first CO_2, the remaining oxygen atom is chemisorbed to the active centre which can oxidize CO through the ER mechanism. For this reaction, the optimized initial state (IS2) is shown in Fig. 4 where CO is just interacting with the Au@g-C_3N_4 surface placed around 3.45 Å from the adsorbed O atom. This initial structure proceeds through a transition state (TS3) and form the final state (FS2) where the CO_2 is adsorbed over the catalyst. In the transition state, CO is located at a distance of 3.237 Å from the O atom. In the optimized FS, CO_2 is physisorbed over the catalyst as discussed in previous section. Here also, we considered 8 images between the initial and final states for NEB calculation and Dimer method is used to locate the exact transition state. Interestingly, this step of the reaction is found to proceed through very low energy barrier of 2.73 kJ/mol. From these results, it can be concluded that the initial CO oxidation over Au@g-C_3N_4 through LH mechanism is the rate limiting step whereas the following step by ER mechanism is almost barrier less.

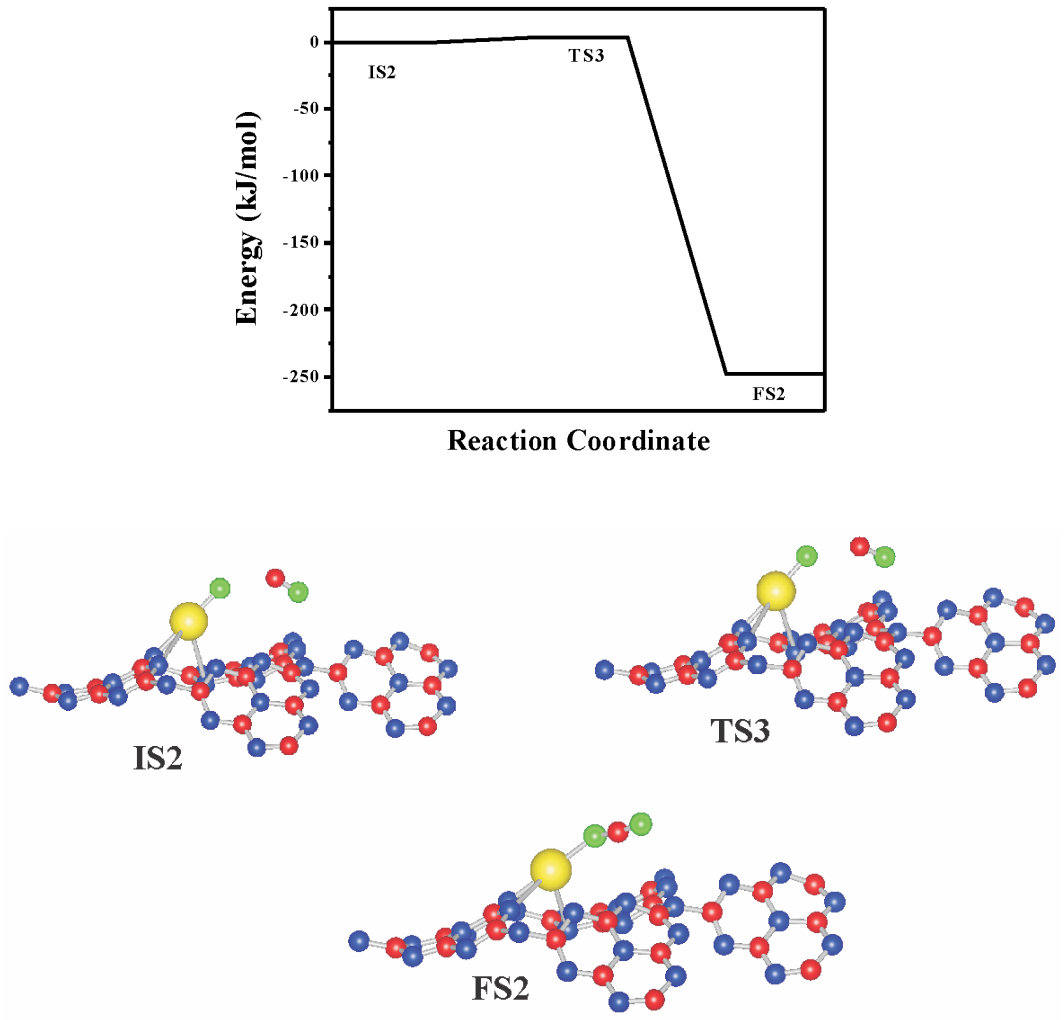

Fig. 4. Energy profiles in the ER mechanism along with the corresponding optimized states (IS2, TS3, and FS2).

Conclusions

In summary, we carried out a systematic first principles study of CO oxidation over the atomic Au decorated g-C_3N_4. Strong binding of Au over the carbon nitride surface reveals its stability against the aggregation of metal atoms to form clusters. Binding energy of both the reactants is found to be considerably higher as compared to that of the product. Molecular oxygen is found to interact with the catalyst through physisorption and the initial step of the CO oxidation is shown to proceed through a Langmuir-Hinshelwood (LH) mechanism followed by Eley-Rideal (ER) mechanism. The largest energy barrier for LH mechanism is found to be 44.19 kJ/mole while it is just 2.73 kJ/mol in the case of ER mechanism.

Acknowledgements

AK thanks HBCSC for NIUS summer research fellowship. We thank the BARC computer centre for providing the high performance parallel computing facility. We also thank Dr. T. K. Ghanty for his continues encouragement and support.

References

1. M. V. Twigg, *Appl. Catal. B,* 2007, **70**, 2.
2. D. R. Merrill and C. C. Scalione, *J. Am. Chem. Soc.,* 1921, **43**, 1982.
3. H. Falsig, B. Hvolbæk, I. S. Kristensen, T. Jiang, T. Bligaard, C. H. Christensen and J. K. Nørskov, *Angew. Chem. Int. Ed.*, 2008, **47**, 4835.
4. R. Prasad and P. Singh, *Catalysis Reviews*, 2012, **54**, 224.

5. X. Xie, Y. Li, Z. Liu, M. Haruta and W. Shen, *Nature,* 2009, **458**, 746.
6. M. S. Chen, Y. Cai, Z. Yan, K. K. Gath, S. Axnanda and D. W. Goodman, *Surf. Sci*., 2007, **601**, 5326.
7. C. Stampfl and M. Scheffler, *Phys. Rev. Lett*., 1997, **78**, 1500.
8. A. Alavi, P. Hu, T. Deutsch, P. L. Silvestrelli and J. Hutter, *Phys. Rev. Lett*., 1998, **80**, 3650.
9. C. J. Zhang and P. Hu, *J. Am. Chem. Soc.,* 2001, **123**, 1166.
10. C. Xu, J. Su, X. Xu, P. Liu, H. Zhao, F. Tian and Y. Ding, *J. Am. Chem. Soc.,* 2007, **129**, 42.
11. L. D. Socaciu, J. Hagen, T. M. Bernhardt, L. Wöste, U. Heiz, H. Häkkinen and U. Landman, *J. Am. Chem. Soc.,* 2003, **125**, 10437.
12. N. K. Jena, K. R. S. Chandrakumar and S. K. Ghosh, *J. Phys. Chem. Lett*., 2011, **2**, 1476.
13. N. Lopez and J. K. Nørskov, *J. Am. Chem. Soc.,* 2002, **124**, 11262.
14. N. Lopez, T. V. W. Janssens, B. S. Clausen, Y. Xu, M. Mavrikakis, T. Bligaard and J. K. Nørskov, *J. Catal*., 2004, **223**, 232.
15. M. Comotti, W. Li, B. Spliethoff and F. Schüth, *J. Am. Chem. Soc*., 2006, **128**, 917.
16. H. H. Kung, M. C. Kung and C. K. Costello, *J. Catal*., 2003, **216**, 425.
17. U. Heiz, A. Sanchez, S. Abbet and W.-D. Schneider, *J. Am. Chem. Soc*., 1999, **121**, 3214.
18. B. Qiao, A. Wang, X. Yang, L. F. Allard, Z. Jiang, Y. Cui, J. Liu, J. Li and T. Zhang, *Nat. Chem*., 2011, **3**, 634.
19. Y. Wang, D. Mei, V. Glezakou, J. Li and R. Rousseau, *Nat. Commun.,* 2015, **6**, 6511.
20. X. F. Yang, A. Wang, B. Qiao, J. Li, J. Liu and T. Zhang, *Acc. Chem. Res*., 2013, **46**, 1470.
21. S. Wang, A. Y. Borisevich, S. N. Rashkeev, M. V. Glazoff, K. Sohlberg, S. J. Pennycook and S. T. Pantelides, *Nat. Mater*., 2004, **3**, 143.
22. G. Kyriakou, M. W. Boucher, A. D. Jewell, E. A. Lewis, T. J. Lawron, A. E. Baber, H. L. Tierney, M. Flytzani-Stephanopoulos and E. C. Sykes, *Science*, 2012, **335**, 1209.
23. Y. Li, Z. Zhou, G. Yu, W. Chen and Z. Chen, *J. Phys. Chem. C*, 2010, **114**, 6250.
24. C. Li, S. Yang, S. Li, J. Xia and J. Li, *J. Phys. Chem. C,* 2013, **117**, 483.
25. P. Zhang, X. F. Chen, J. S. Lian and Q. Jiang, *J. Phys. Chem. C,* 2012, **116**, 17572.
26. P. Munnik, P. E. de Jongh and K. P. de Jong, *Chem. Rev*., 2015, **115**, 6687.
27. J. Dai, J. Song, Y. Qiu, J. Wei, Z. Hong, L. Li and H. Yang, *ACS Appl. Mater. Interfaces,* 2019, **11**, 10589.
28. S. Lin, X. Ye, R. S. Johnson and H. Guo, *J. Phys. Chem. C,* 2013, **117**, 17319.
29. K. Almeida, P. Pena, T. B. Rawal, W. C. Coley, A. Akhavi, M. Wurch, K. Yamaguchi, D. Le, T. S. Rahman and L. Bartels, *J. Phys. Chem. C,* 2019, **123**, 6592.
30. P. Wu, P. Du, H. Zhang and C. Cai, *Phys. Chem. Chem. Phys.,* 2015, **17**, 1441.
31. K. Srinivasu and S. K. Ghosh, *J. Phys. Chem. C,* 2013, **117**, 26021.
32. A. V. Krasheninnikov, P. O. Lehtinen, A. S. Foster, P. Pyykkö and R. M. Nieminen, *Phys. Rev. Lett.,* 2009, **102**, 126807.
33. X. Wang, K. Maeda, A. Thomas, K. Takanabe, G. Xin, J. M. Carlsson, K. Domen and M. Antonietti, *Nat. Mater*., 2008, **8**, 76.
34. H. Pan, Y. W. Zhang, V. B. Shenoy and H. Gao, *ACS Catal*., 2011, **1**, 99.
35. W. Ong, L. Tan, Y. Hau Ng, S. Yong and S. Chai, *Chem. Rev.,* 2016, **116(12)**, 7159.
36. K. Srinivasu, B. Modak and S. K. Ghosh, *J. Phys. Chem. C,* 2014, **118**, 26479.
37. K. Srinivasu and S. K. Ghosh, *J. Mater. Chem. A,* 2015, **3**, 23011.
38. K. Srinivasu, B. Modak and S. K. Ghosh, *Phys. Chem. Chem. Phys.,* 2016, **18**, 26466.
39. S. Samanta, S. Martha and K. Parida, *ChemCatChem,* 2014, **6**, 1453.
40. M. E. Khan, T. H. Han, M. M. Khan, M. R. Karim and M. H. Cho, *ACS Appl. Nano Mater.,* 2018, **1**, 2912.
41. H. Wang, T. Sun, L. Chang, P. Nie, X. Zhang, C. Zhao and X. Xue, *Electrochimica Acta,* 2019, **303**, 110.
42. G. Kresse and J. Furthmüller, *Phys. Rev. B,* 1996, **54**, 11169.
43. G. Kresse and J. Furthmüller, *Comput. Mater. Sci.,* 1996, **6**, 15.
44. G. Kresse and D. Joubert, *Phys. Rev. B,* 1999, **59**, 1758.
45. P. E. Blöchl, *Phys. Rev. B,* 1994, **50**, 17953.
46. J. P. Perdew, K. Burke and M. Ernzerhof, *Phys. Rev. Lett*., 1996, **77**, 3865.
47. S. Grimme, *J. Comput. Chem*., 2006, **27**, 1787.
48. H. J. Monkhorst and J. D. Pack, *Phys. Rev. B,* 1976, **13**, 5188.
49. G. Henkelman and H. Jónsson, *J. Chem. Phys.,* 2000, **113**, 9901.
50. G. Henkelman and H. Jónsson, *J. Chem. Phys.,* 2000, **113**, 9978.
51. J. Kästner and P. Sherwood, *J. Chem. Phys.,* 2008, **128**, 014106.
52. G. Henkelman and H. Jónsson, *J. Chem. Phys.,* 1999, **111**, 7010.
53. A. Heyden, A. T. Bell and F. J. Keil, *J. Chem. Phys.,* 2005, **123**, 224101.
54. K. Momma and F. Izumi, *J. Appl. Crystallogr.*, 2008, **41**, 653.
55. W. Tang, E. Sanville and G. Henkelman, *Condens. Matter*, 2009, **21**, 084204.